Ann. Geophys., 24, 2901–2909, 2006
www.ann-geophys.net/24/2901/2006/

Annales Geophysicae

The relationship between small-scale and large-scale ionospheric electron density irregularities generated by powerful HF electromagnetic waves at high latitudes

E. D. Tereshchenko[1], B. Z. Khudukon[1], M. T. Rietveld[2], B. Isham[3], T. Hagfors[4], and A. Brekke[5]

[1]Polar Geophysical Institute, 15 Khalturina St. 183010 Murmansk, Russia
[2]EISCAT Scientific Association, 9027 Ramfjordbotn, Norway
[3]Interamerican University, Bayamón, Puerto Rico 00957, USA
[4]Max Planck Institute for Solar System Research, 37191 Katlenburg-Lindau, Germany
[5]University of Tromsø, 9037 Tromsø, Norway

Received: 3 April 2006 – Accepted: 27 June 2006 – Published: 21 November 2006

Abstract. Satellite radio beacons were used in June 2001 to probe the ionosphere modified by a radio beam produced by the EISCAT high-power, high-frequency (HF) transmitter located near Tromsø (Norway). Amplitude scintillations and variations of the phase of 150- and 400-MHz signals from Russian navigational satellites passing over the modified region were observed at three receiver sites. In several papers it has been stressed that in the polar ionosphere the thermal self-focusing on striations during ionospheric modification is the main mechanism resulting in the formation of large-scale (hundreds of meters to kilometers) nonlinear structures aligned along the geomagnetic field (magnetic zenith effect). It has also been claimed that the maximum effects caused by small-scale (tens of meters) irregularities detected in satellite signals are also observed in the direction parallel to the magnetic field. Contrary to those studies, the present paper shows that the maximum in amplitude scintillations does not correspond strictly to the magnetic zenith direction because high latitude drifts typically cause a considerable anisotropy of small-scale irregularities in a plane perpendicular to the geomagnetic field resulting in a deviation of the amplitude-scintillation peak relative to the minimum angle between the line-of-sight to the satellite and direction of the geomagnetic field lines. The variance of the logarithmic relative amplitude fluctuations is considered here, which is a useful quantity in such studies. The experimental values of the variance are compared with model calculations and good agreement has been found. It is also shown from the experimental data that in most of the satellite passes a variance maximum occurs at a minimum in the phase fluctuations indicating that the artificial excitation of large-scale irregularities is minimum when the excitation of small-scale irregularities is maximum.

Correspondence to: M. T. Rietveld
(mike.rietveld@eiscat.uit.no)

Keywords. Ionosphere (Active experiments; Ionospheric irregularities) Radio scinece (Ionospheric physics)

1 Introduction

One very effective method for studying physical processes in the ionosphere is to perturb the ionospheric medium using a powerful HF radio wave, or pump. The resulting fast heating of the plasma causes significant changes in the energy distribution of ionospheric electrons and the resulting instabilities can provide appropriate conditions for the generation of artificial ionospheric electron density irregularities. Experimental studies of these effects can be found in many works, e.g., in the papers by Gurevich (1978), Basu et al. (1987), Stubbe (1996), Costa et al. (1997), Gurevich et al. (2002), Tereshchenko et al., (1998, 2000a, 2000b). The observations show that electron density irregularities with scales ranging from meters up to tens of kilometers can be produced in the ionosphere by HF pumping. The irregularities produce artificial spread F seen on HF ionograms, scintillations on HF and VHF signal paths from radio stars and satellite beacons propagating through the modified region, artificial field-aligned scattering, and wide-band attenuation of HF radio waves in the disturbed region (Rietveld et al., 1993; Gurevich et al., 2002).

It was suggested by Gurevich (1978) and Gurevich et al. (1998, 2002) that the thermal resonance self-focusing instability is the main mechanism for producing electron density irregularities as a result of focusing and defocusing a pump wave in the region of density perturbations caused by the wave. In brief, the self-focusing instability developing in the upper hybrid plasma resonance region leads to formation of closely packed small-scale structures which are bundles of meter- to decameter-sized field-aligned plasma

Published by Copernicus GmbH on behalf of the European Geosciences Union.

density structures, or striations, containing a high electron temperature and a reduced average electron density. This reduced average density during the excitation of a large number of striations results in a new nonlinear process – self-focusing on the striations in the pump wave. This process is strongly anisotropic in the plane perpendicular to the magnetic field. In the polar ionosphere these closely packed nonlinear structures form large-scale irregularities which are aligned along the geomagnetic field. A powerful pump wave may be trapped in these nonlinear structures and propagate along the magnetic field in the magnetic zenith direction. One such nonlinear structure, a soliton-type solution describing "bunches" of striations and the resulting soliton-like pump-wave field distribution, was described by Gurevich et al. (1998). Strong Ohmic heating of the ionospheric plasma by the trapped wave leads to the creation of large-scale (hundreds of meters to kilometers) irregularities.

Much of the recent experimental and theoretical work on the dependence of HF-generated irregularities and electron energisation such as that in Gurevich et al. (2002) was prompted by the discovery of the magnetic zenith effect, which is the observation that radio-induced optical emissions are preferentially observed close to the magnetic zenith direction seen from the transmitter (Kosch et al., 2000; Pedersen and Carlson, 2001) even when the main beam of the HF transmitter was pointed in other directions. A closely related phenomenon was the discovery that HF-enhanced ion and plasma lines observed using the EISCAT UHF incoherent scatter radar were strongest when the radar was pointing close to the magnetic zenith even when the HF beam was not (Isham et al., 1999). Also electron temperature enhancements were found to be strongest for field-aligned HF rays (Rietveld et al., 2003). In addition, some preliminary measurements suggest that stimulated electromagnetic emissions induced in the ionospheric F region come from directions close to field-aligned (Isham et al., 2005; Tereshchenko et al., 2006). Because HF-induced small scale electron density irregularities are thought to be closely linked to HF-induced electron temperature increases through a thermal parametric instability (e.g. Robinson, 1989), and because they are associated with the SEE phenomenon, it is interesting to try to examine whether the irregularities are also distributed in space near the heated region in the same way as the optical emissions, electron temperatures, enhanced plasma waves and stimulated emissions.

The work by Gurevich et al. (2002) concentrates only on the phase fluctuations of satellite radio signals during HF pumping, caused mostly by large-scale irregularities. In contrast, the small-scale irregularities (tens of meters) mainly affect radio amplitude scintillations (Tereshchenko et al., 2000a, 2000b). In the present paper we use a statistical approach in describing scatter from small-scale irregularities (Kunitsyn and Tereshchenko, 2003; Tereshchenko et al., 1999, 2000a, 2004a), and the relation between the variance of the logarithmic relative amplitude of the scattered radio wave and the parameters of scattering irregularities in the high latitude ionosphere is obtained. In most of the cases in our data set it was found that the amplitude scintillation maxima do not exactly correspond to where the difference between the field-aligned direction and the line-of-sight to the satellite is a minimum. Phase fluctuations are also studied in the present paper to estimate the relationship between small-scale and large-scale irregularities induced by powerful HF transmissions. The experimental results obtained during six satellite passes over the receiver chain are presented.

2 Description of the experiment

The experimental data used in the analysis presented here were obtained during an HF-tomographic campaign carried out from 5 to 17 June, 2001, using the EISCAT HF transmitter facility located at Ramfjordmoen near Tromsø, Norway (69.59° N, 19.22° E) (Rietveld et al., 1993). The low frequency (4.0–5.5 MHz) low-gain antenna array (23 dBi at the mid-frequency of the full array) was used to continuously pump a region located nearly directly overhead for about 12 min during each of six satellite passes. The EISCAT 929-MHz (UHF) incoherent scatter radar made standard ion-line measurements, including tristatic reception (at Tromsø, Norway; Kiruna, Sweden; and Sodankylä, Finland) in many but not all cases. The relevant experimental parameters are given in Table 1.

Three satellite receivers were installed under the modified region on a chain lying approximately along or parallel to the north-to-south satellite passes, thereby making it possible to study the temporal features and the spatial electron density distribution both in the F and E regions, within and outside the cone of the HF antenna beam. The central site was at Ramfjordmoen (69.59° N, 19.22° E), the northern station at Futrikelv (69.80° N, 19.02° E), and the southern site at Seljelvnes near Nordkjosbotn (69.25° N, 19.43° E), with a spacing of about 25 km between Futrikelv and Ramfjordmoen and 39 km between Ramfjordmoen and Seljelvnes (the receiver site at Ramfjordmoen, which is co-located with the HF and radar transmitters, is the same as the site called "Tromsø" in Tereshchenko et al., 2000a and 2000b). In total about 20 records from the Russian satellites were made at each site during the HF experiments. The receivers measured radio signals from Russian navigational satellites orbiting at about 1000 km, with orbital inclinations of 83° and periods of 105 min. Only passes of satellites with such a high elevation that they could cross the ionospheric region illuminated by the main lobe of the HF antenna were used in the analysis. The mobile automatic receiving systems used to measuring the relative phase between the 150-MHz (VHF) and 400-MHz (UHF) satellite beacon signals and the amplitude of the 150-MHz signal (Kunitsyn and Tereshchenko, 2003) were constructed and deployed by the Polar Geophysical Institute. The period of the observations turned out to

Table 1. Parameters of the satellite data and HF operation modes.

Modification session number	Time interval of the studied satellite records [UT]	Coordinates of the satellite at maximum elevation		Modification time interval [UT]	HF pump parameters beam pointing: 0º vertical, + to North, – to South
		Azimuth [deg]	Maximum elevation [deg]		
1	07.06.2001 20:15:38-20:20:37	106°	85°	20:12-20:24	5.423 MHz, O-mode, 230 MW, CW, 0º pointing
2	10.06.2001 18:03:41-18:08:40	89°	84°	18:00-18:12	4.9128 MHz, O-mode, 144 MW, CW, –6º pointing
3	10.06.2001 19:54:53-20:00:42	111°	85°	19:51-20:03	4.9128 MHz, O-mode, 138 MW, CW, –12º pointing
4	13.06.2001 17:51:49-17:57:18	158°	87°	17:48-18:01	4.9128 MHz, O-mode, 181 MW, CW, –6º pointing
5	13.06.2001 19:34:07-19:39:36	115°	85°	19:30-19:43	4.9128 MHz, O-mode, 183 MW, CW, –6º pointing
6	16.06.2001 17:40:03-17:45:32	236°	84°	17:36-17:49	5.423 MHz, O-mode, 233 MW, CW, –6º pointing

be favorable for investigating artificial irregularities, because the natural ionosphere was regular and the geomagnetic activity was low.

Figure 1 presents the satellite trajectory for the pass on 13 June 2001 at 17:52 UT, along with the HF antenna pattern (the solid bold contour) and the contours of Θ, the angle between the line-of-sight from a satellite to the receiver at Ramfjordmoen and the geomagnetic field direction (the dashed contours) at 300 km altitude above Ramfjordmoen. The contours of Θ show the locus of the angle Θ for satellite passes near the heated region. The notation Θ has also been used in previous papers. The square shows the position of the maximum variance of the logarithmic relative amplitude measured at Ramfjordmoen. The satellite position of closest approach on this southward pass was 89.9° elevation and 125° azimuth. The heating interval was 17:48–18:00 UT, with a 4.9128 MHz O-mode continuously-transmitted HF pump wave and an antenna beam width of 11.8° directed 6° to the south.

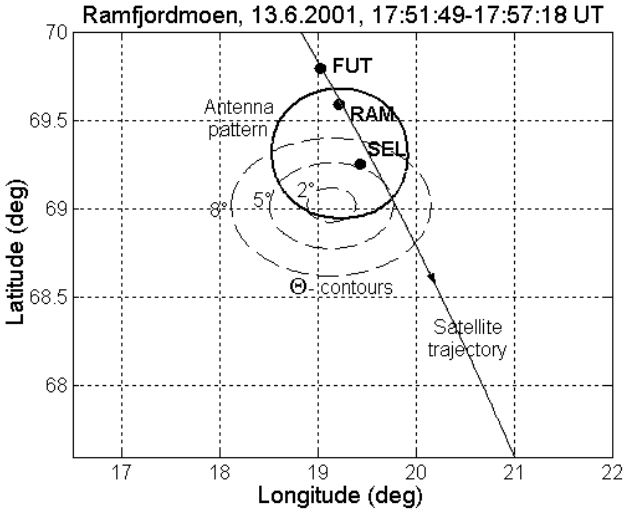

Fig. 1. The satellite trajectory, HF antenna pattern (the solid bold contour), and contours of the Θ-angle for a receiver at Ramfjordmoen (the dashed lines), at 300 km altitude. The square shows that the position of the level of the variance maximum is at Θ=8° as measured at the Ramfjordmoen receiver, rather than the expected Θ=5° (in the absence of anisotropies). The satellite track segment shown here covers only part of the time interval indicated at the top.

3 Experimental results

As mentioned earlier, amplitude scintillations can be described by σ_χ^2, the variance of the logarithmic relative amplitude of the scattered radio wave (Kunitsyn and Tereshchenko, 2003; Tereshchenko et al., 1998, 1999, 2000b). Here

$$\chi = \ln(A / A_0) \quad (1)$$

where A is the observed amplitude after passing through the irregularity region, A_0 is the amplitude of undisturbed field (without irregularities), and χ is the logarithmic relative amplitude of A. Then

$$< A >= A_0 \exp\left(-\frac{1}{2}\sigma_\chi^2\right), \quad (2)$$

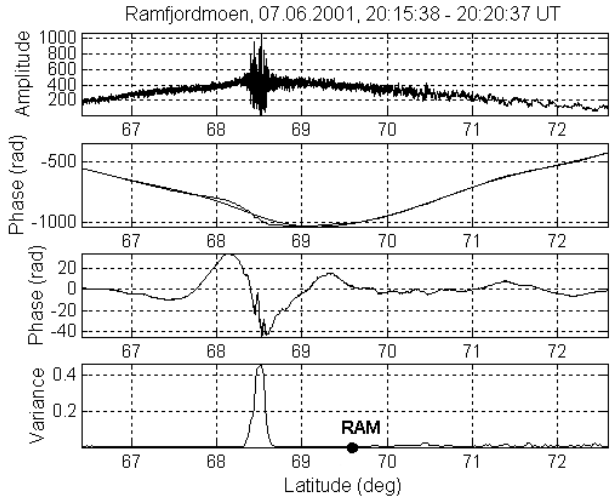

Fig. 2. Amplitude (top panel), phase and smoothed phase (second panel from top), phase fluctuations (third panel) and amplitude variance (variance of the logarithmic relative amplitude fluctuations) (bottom panel). The variance averaging interval is 6 s, while the phase is plotted at the 50 Hz-sampling rate of the raw data.

where the angular brackets indicate the statistical average. The average amplitude $<A>$ and the variance σ_χ^2 are thus quantitative measures of the amplitude variations which characterize the probe wave after passing through the irregularity region. The amplitude variance curve has a distinct maximum when small-scale irregularities exist in the ionosphere (Tereshchenko et al., 2000a).

Figure 2 shows an example of the amplitude, raw phase, smoothed and de-trended phase, and variance of the logarithmic relative amplitude fluctuation of the satellite signal at Ramfjordmoen on 7 June 2001 at 20:20:37 UT during HF pumping. It can be seen that the minimum of the phase fluctuations (due to large-scale irregularities) at 68.6° coincides with the largest amplitude scintillations (due to small-scale irregularities) and the corresponding variance maximum. This correspondence between the minimum in the phase fluctuations and the variance maximum is confirmed by further examples in Fig. 3 where six satellite passes are presented.

The receiver sites Futrikelv, Ramfjordmoen, and Seljelvnes are indicated in the figure as FUT, RAM, and SEL. The smooth bold lines on the bottom panels of Fig. 3 show the Θ-angle. The plots display the variation of the variance of the logarithmic relative amplitude fluctuations observed at the three sites. It can be seen that in about 12 out of the 18 plots the variance peak occurs near a minimum in phase. The approximate number arises because some cases are not so clear, as when there are rapid phase fluctuations. Taking into account that the phase fluctuations are obtained from the integral phase, it should be noted that the minimum can also be hidden in an irregular medium and may not be so clearly seen, as for example the pass on 13 June 2001 from 19:34 to 19:40 UT.

It was mentioned above that ionospheric conditions were quiet during the experiment. This situation makes it possible to study whether artificial irregularities are preferentially excited in the field-aligned direction. An important result illustrated in Fig. 3 is that the scintillation maximum (the variance peak in the lower panels) was generally not observed to coincide with the direction nearest to field-aligned (the minimum in the Θ-curves in the lower panels). In order to explain this effect let us consider the spectrum of the irregularities which can be written as

$$\Phi(\boldsymbol{\kappa}, z) = \sigma_N^2(z)\, \Phi_N(\boldsymbol{\kappa}, z), \tag{3}$$

where $\Phi_N(\boldsymbol{\kappa}, z)$ is the normalized spectral density and $\sigma_N^2(z)$ is the variance of electron density fluctuations. In most investigations of the ionospheric irregularity spectrum, a power-law spectrum is taken to be the most suitable approximation for describing the irregularities. This spectrum can be written as follows (Kunitsyn and Tereshchenko, 2003, Tereshchenko et al., 1999):

$$\Phi_N(\boldsymbol{\kappa},\ z) = \frac{\alpha\,\beta\,L_0^3\,\Gamma\left(\frac{p}{2}\right)}{2\pi\,\Gamma(3/2)\,\Gamma\left[(p-3)/2\right]}$$

$$\left[1+\left(\frac{L_0}{2\,\pi}\right)^2\left(\alpha^2\kappa_{\,||}^{\,2}+\beta^2\kappa_x^2+\kappa_y^2\right)\right]^{-\frac{p}{2}} \tag{4}$$

In this formula Γ is the gamma function, p is the power index, L_0 is the scale size of the irregularities, $k_{||}$, k_x, and k_y are the wave vector $\boldsymbol{k}$ components parallel ($k_{\,||}$) and perpendicular (k_x, k_y) to the propagation direction, and α and textit β are the anisotropy axial ratios, or elongations, of the irregularities in the planes parallel and perpendicular to the geomagnetic field; thus α and β have values greater than or equal to one. The above equation gives the expression for the variance of the logarithmic relative amplitude fluctuations as follows:

$$\sigma_\chi^2 = \frac{\lambda^2 r_e^2}{4\pi^2}\int_{z_u}^{z_d}\int_{-\infty}^{\infty}\int \Phi_N(\boldsymbol{\kappa}, z)\,|_{\kappa_z=0}\sin^2\frac{R_F^2(\kappa_x^2+\kappa_y^2)}{4\pi}d\boldsymbol{\kappa}_x d\boldsymbol{\kappa}_y dz, \tag{5}$$

where $R_F = [\lambda\, z\,(z_0-z)/z_0]^{1/2}$ is the radius of the principal Fresnel zone, λ is the wave length, r_e=2.82·10^{-15} m is the classical electron radius, and z_o is the distance between the satellite and the receiver, and where the z-axis is along the line of sight from satellite to receiver (identical to the parallel direction of Eq. 4). The small-scale irregularities are assumed to lie between the satellite and the receiver confined by the region z_u<z<z_d. Here z_u and z_d are the boundaries of the irregular layer. The signal strength observed on the ground is affected by irregularities scattering at or close to the z axis. The slowly varying Fresnel radius can be easily

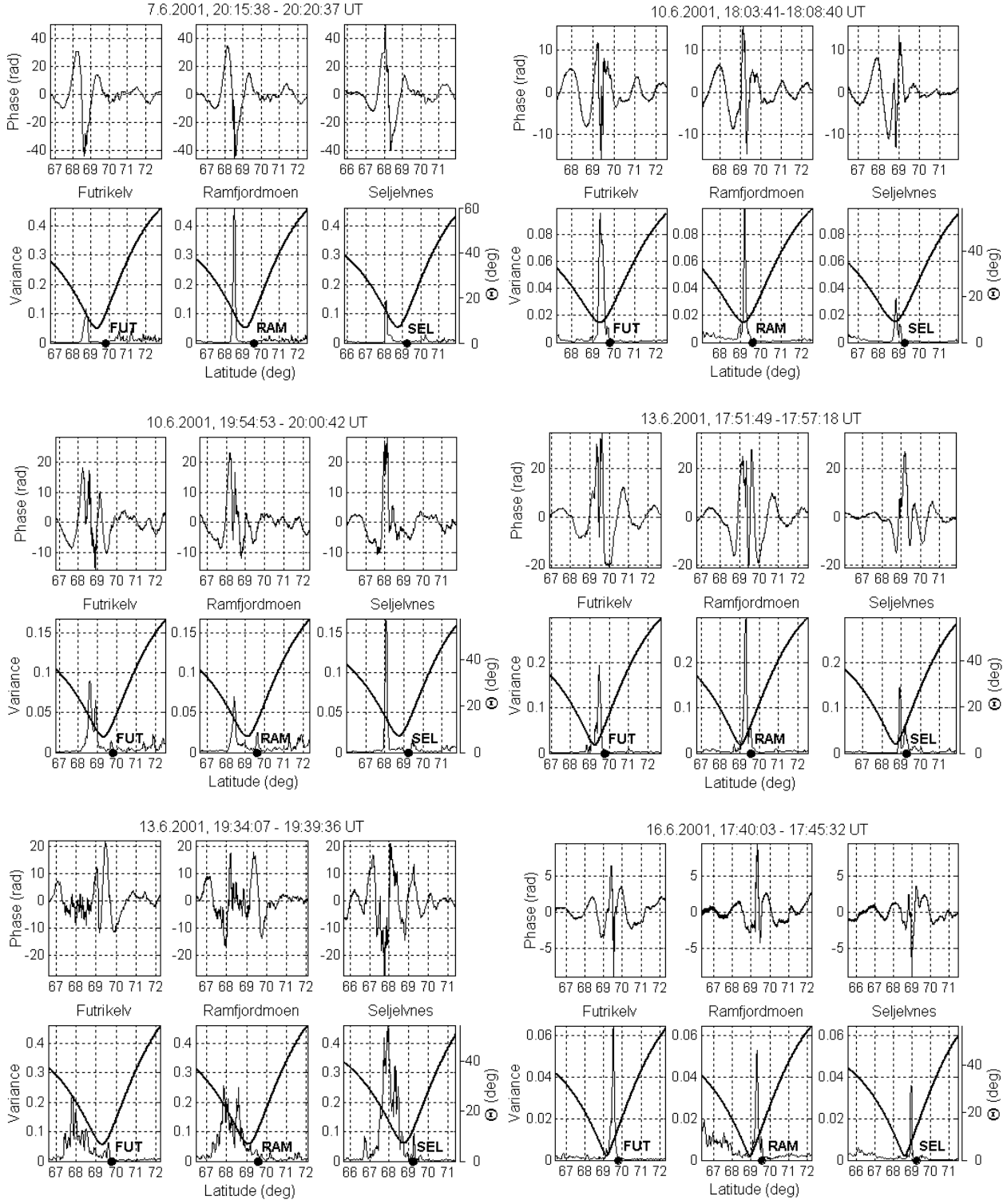

Fig. 3. Six satellite passes during heating. The phase fluctuations (upper panels), and the variance of the logarithmic relative amplitude fluctuations and Θ-angle (lower panels) are shown. The Y-axis at the right end of the lower right plot for each pass shows the Θ-scale in degrees (the same scale for each station). The variance averaging interval is 6 s, while the phase is plotted at the 50 Hz-sampling rate of the raw data.

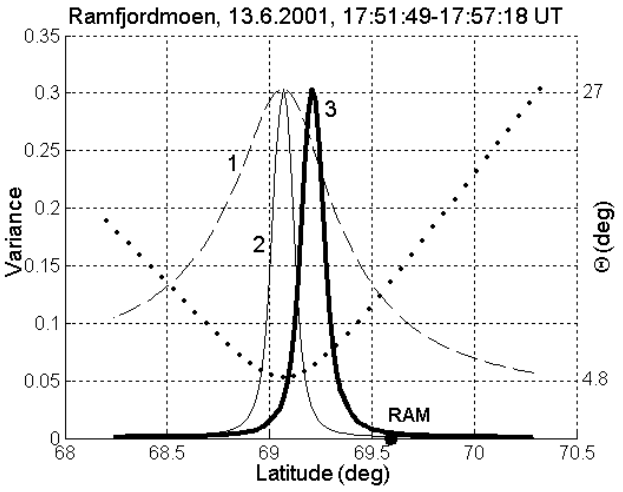

Fig. 4. The power law spectrum variance of the logarithmic relative amplitude fluctuations at Ramfjordmoen (curves 1 to 3) calculated for the Θ-angle (dots) corresponding to the orbital parameters of the satellite pass on 13 June 2001 at 17:51:49 UT.

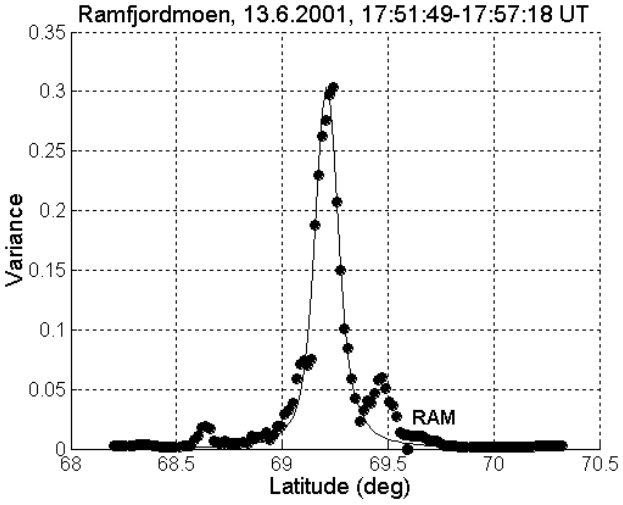

Fig. 5. Comparison between the experimental variance (the dots) and its model curve (the solid line which is curve 3 in the previous figure). The Ramfjordmoen data shown here for 13 June 2001 are within but not fully covering the interval indicated at the top.

calculated for each satellite trajectory and the Θ-angle is obtained from the magnetic field model. Therefore σ_χ^2 can be calculated for given values of the anisotropy parameters and a given model of $\sigma_N^2(z)$. The anisotropic parameters can be determined by varying their values until the best fit to the experimental curve is obtained. The variance expressed in Eq. (5) varies with the satellite latitude in an implicit form being dependent on the angle between the line of sight from satellite to receiver and the field direction as well as on the anisotropy parameters of the irregularities (Tereshchenko et al., 1999).

Figure 4 presents the calculation results of σ_χ^2 for the power law spectrum (curves 1 to 3) and the Θ-angle (dots) using the geometry parameters of the satellite pass on 13 June 2001 at 17:52 UT for the Ramfjordmoen site. The variance averaging interval used is also 6 s and the ionospheric height H_i is 300 km. Curve 1 corresponds to irregularities perpendicular to the geomagnetic field line, with perpendicular axial ratio β=1, indicating that the irregularity is isotropic in the perpendicular plane, and parallel axial ratio α=63. The maximum of curve 2 corresponds to the Θ-angle minimum and an orientation angle of the transverse axis (the x axis in Eq. 3) relative to the north direction of ∼70°, meaning that in the plane perpendicular to the geomagnetic field line the irregularity is elongated along an axis offset just 20° from the east-west direction. The magnitude of this elongation is given by β=11, while the parallel axial ratio α was set to 63. Curve 3 (bold) corresponds to the experimental data (see Fig. 5) with the orientation angle of the transverse axis equal to 37° relative to the north direction and with the same β=11 and α=63. In this case the minimum angle of the line-of-sight to the satellite and the geomagnetic field line is 4.8° but the location of the variance maximum is 5.6°.

It can be seen that the anisotropy of the small-scale irregularities in the plane perpendicular to the geomagnetic field clearly influences the deviation of the variance maximum relative to the magnetic field direction. This allows us to use the observed position of the variance maximum to deduce the anisotropy axis direction, and the width of the curve to deduce the degree of anisotropy in the plane perpendicular to the magnetic field. As one of the possible reasons, this effect might be caused by large drifts in the polar ionosphere producing an anisotropy of the small-scale irregularities in a direction perpendicular to the geomagnetic field. The deviation of the variance maximum might also seem to be due to refraction of the satellite signals or HF wave, however no strong gradients of the electron density were observed. The lack of gradients was deduced from analysis of the phase from satellite passes before and after heating during summer natural conditions. The phase of the satellite signals is a sensitive indicator of strong gradients. In addition, the measured curves of the variance σ_χ^2 are quite narrow, which is a typical feature of an anisotropic spectrum (Kunitsyn and Tereshchenko, 2003). Figure 5 shows a comparison between the experimental variance values (the dots) for this satellite pass on 13 June 2001 at 17:52 UT and the modeling curve (the solid line). Quite good agreement between the curves is clearly seen.

3.1 Comparison with drift velocities

The EISCAT UHF radar was operated during most of these satellite passes in a tristatic configuration, allowing accurate

Table 2. Anisotropy directions compared to EISCAT velocities. Both directions are measured clockwise from north.

Date, Time [UT]	Station	Anisotropy parameters				Anisotropy direction (= Ψ+180°) [deg]	EISCAT vector velocity	
		H_i [km]	α/β	Ψ [deg]	θ_{min} [deg]		direction ± std. dev. [deg]	magnitude ± std. dev. [m/s]
10.06.2001, 18:03:41 – 18:08:40	Futrikelv	300	5	72°	9.9°	252°	200° ±7°	424 ±105
	Ramfjordmoen		5	71°	10°	251°		
	Seljelvnes		5	72°	10.2°	252°		
10.06.2001, 19:54:53 – 20:00:42	Futrikelv	300	5	80°	8.2°	260°	294° ±22°	227 ±48
	Ramfjordmoen		6.4	97°	8.3°	277°		
	Seljelvnes		5.3	92°	8.5°	272°		
13.06.2001, 17:51:49 – 17:57:18	Futrikelv	300	5.7	44°	4.7°	224°		
	Ramfjordmoen		5.7	37°	4.8°	217°		
	Seljelvnes		7	40°	4.9°	220°		
16.06.2001, 17:40:03 – 17:45:32	Futrikelv	300	7.2	153°	0.5°	333°	227° ±21°	187 ±93
	Ramfjordmoen		8.3	154°	0.6°	334°		
	Seljelvnes		9.0	154°	0.6°	334°		

estimates of the 3-D plasma drift velocity. It is interesting to compare the direction of these drifts with the irregularity anisotropy direction found from the analysis above. The intersection volume of the Tromsø, Kiruna, and Sodankylä antenna beams was at 295 km along the magnetic field line through Tromsø. The long pulse of the cp1l modulation was used to obtain three line-of-site velocities which were combined to obtain the vector velocity. Data from all three radar sites were obtained on three of the satellite passes: the two on 10 June 2001 and the one on 16 June 2001. On 13 June 2001 only Tromsø and Kiruna data were available for the 17:52 UT pass so that the vector velocities obtained were unreliable.

Figure 6 shows the velocity vectors obtained every minute together with the irregularity anisotropy directions from the variance analysis for the approximately 6-min interval as outlined above. There is general agreement between the velocity and anisotropy directions even though the velocities were somewhat variable. Some difference between the directions may be expected because of the fairly large distance between the EISCAT common volume and the scintillations measured. The results of the variance analysis and vector velocities from EISCAT are summarised in Table 2. The velocities are the average of the one-minute average velocities with ± indicating the standard deviations. The anisotropy directions agree fairly well with the average EISCAT velocities, especially when one considers that the volumes of measurement are not identical, separated in the case of Fig. 6 by up to 42 km in the north-south and 59 km in the east-west

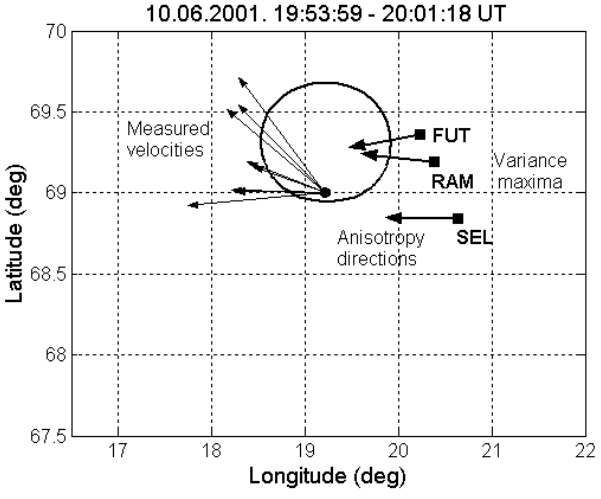

Fig. 6. Map showing the pump antenna pattern (the nearly circular contour), and the position of velocity measurements by the EISCAT UHF radar (the dot) with six one-minute averaged tristatic velocities measured on 10 June 2001 between 19:53:59 and 20:01:18 UT (arrows), and variance maxima locations (the squares) and anisotropy directions (the bold solid arrows) corresponding to the Futrikelv, Ramfjordmoen and Seljelvnes sites for the approximately 6-min time period all at 300 km. The largest UHF tristatic velocity vector corresponds to 280 m/s whereas the anisotropy vector magnitudes are arbitrary.

directions, up to 93 and 74 km in the case of 10 June 2001 18:02:59–18:10:59 UT, and up to 61 and 27 km in the case of 16 June 2001 17:40:03–17:45:32 UT, thus confirming the results found in Tereshchenko et al. (2000b).

3.2 Magnetic zenith effect

The variance peaks in Fig. 3 occur at latitudes both above and below that corresponding to field-aligned which is 69.0°. If we consider only the variance peaks for Ramfjordmoen, we find that for three of the passes the peak occurs south of field-aligned (the minimum of the Θ curve), two occur north of field-aligned and one occurs at the field-aligned position. There is also no correlation of the position of the variance maximum with HF beam pointing either. The largest variance of the three sites was measured at Ramfjordmoen in three out of the six passes. A clear magnetic zenith effect should manifest itself as a preference for the variance peak to occur close to the field-aligned position at 69.0° N latitude but this is not observed in our data. The main reason for this is likely to be the effect of the irregularity anisotropy as described earlier which can make the variance peak appear at different parts of the satellite track. Therefore we cannot make any conclusions about a possible magnetic zenith effect from our data.

4 Summary

The results of VHF satellite radio probing of the high-latitude ionosphere modified by the powerful transmission from the EISCAT HF heating facility at Ramfjordmoen near Tromsø, Norway, in June 2001 have been described, revealing the generation of both large-scale electron density irregularities and small-scale irregularities during the ionospheric modification. Phase fluctuations of radio signals occur mostly due to large-scale irregularities, whereas small-scale irregularities mainly produce amplitude scintillations. The parameters of the small-scale irregularities have been determined using a statistical method in which the experimental and model variance of the logarithmic relative amplitude fluctuations of VHF satellite signals, which describes the properties of small-scale irregularities, are computed. It has been found that the maximum of the amplitude scintillations does not strictly correspond to the situation where the line-of-sight from the radio source to receiver coincides with the minimum angle between line-of-sight to the satellite and the geomagnetic field direction. One reason could be a close relation between small-scale irregularities anisotropy in a direction perpendicular to the geomagnetic field and ionospheric drifts. The effect is quite noticeable in the high latitude ionosphere where drifts can be large. EISCAT observations of the plasma drift during some of the passes confirm the close alignment between the anisotropy and drift directions. It has been illustrated by a series of satellite passes that in about 12 cases out of 18 the minimum of the phase fluctuations corresponds to the variance maximum, indicating that the excitation of large-scale irregularities is minimum when that for small-scale irregularities is maximum.

Acknowledgements. The authors gratefully acknowledge the support of the EISCAT Scientific Association which made it possible to perform the experiment. EISCAT is an international association supported by Finland (SA), France (CNRS), Germany (MPG), Japan (NIPR), Norway (NFR), Sweden (VR) and the United Kingdom (PPARC). The authors thank N. Yu. Romanova for making model calculations of the variance. The present work was financially supported by the University of Tromsø under the Agreement of the Scientific and Technical Cooperation between the Polar Geophysical Institute of the Russian Academy of Sciences and the University of Tromsø, signed on 24 October 2002. The work was also supported by the INTAS grant 03-51-5583 and by the Russian Foundation of Basic Research grants 03-05-64937 and 03-05-64636.

Topical Editor M. Pinnrock thanks two referees for their help in evaluating this paper.

References

Basu, S., Basu, S., Stubbe, P., Kopka, H., and Waaramaa, J.: Daytime scintillations induced by high-power HF waves at Tromsø, Norway, J. Geophys. Res., 92, 11 149–11 157, 1987.

Costa, E., Basu, S., Livingston, R. C., and Stubbe, P.: Multiple baseline measurements of ionospheric scintillation induced by high-power HF waves, Radio Sci., 32, 1, 191–197, 1997.

Gurevich, A. V.: Nonlinear phenomena in the ionosphere, Springer-Verlag, New York, 1978.

Gurevich, A., Hagfors, T., Carlson, H., Karashtin, A., and Zybin, K.: Self-oscillations and bunching of striations in ionospheric modifications, Phys. Lett A, 239, 385–392, 1998.

Gurevich, A., Fremouw, E., Secan, J., and Zybin, K.: Large scale structuring of plasma density perturbations in ionospheric modifications, Phys. Lett. A, 301, 307–314, 2002.

Isham, B., Rietveld, M. T., Hagfors, T., La Hoz, C., Mishin, E., Kofman, W., Leyser, T. B., and van Eyken, A. P.: Aspect angle dependence of HF enhanced incoherent backscatter, Adv. Space Res., 24, 1003–1006, 1999.

Isham, B., Hagfors, T., Khudukon, B. Z., Yurik, R. Yu., Tereshchenko, E. D., Rietveld, M. T., Belyey, V., Grill, M., La Hoz, C., Brekke, A., and Heinselman, C.: An interferometer experiment to explore the aspect angle dependence of stimulated electromagnetic emission spectra, Ann. Geophys., 23, 55–74, 2005,
http://www.ann-geophys.net/23/55/2005/.

Kosch, M. J., Rietveld, M. T., Hagfors, T., and Leyser, T. B.: High-latitude HF-induced airglow displaced equatorwards of the pump beam, Geophys. Res. Lett., 27, 17, 2817–2820, 2000.

Kunitsyn, V. E. and Tereshchenko, E. D.: Ionospheric tomography, Springer-Verlag, Berlin, 259pp, 2003.

Pedersen, T. R. and Carlson, H. C.: First observations of HF heater-produced airglow at the High Frequency Active Auroral Research Program facility: Thermal excitation and spatial structuring, Radio Sci., 36, 5, 1013–1026, 2001.

Rietveld, M. T., Kohl, H., Kopka, H., and Stubbe, P.: Introduction to Ionospheric Heating at Tromsø – I. Experimental Overview, J. Atmos. Terr. Phys. 55, 577–599, 1993.

Rietveld, M. T., Kosch, M. J., Blagoveshchenskaya, N. F., Kornienko, V. A., Leyser, T. B., and Yeoman, T. K.: Ionospheric electron heating, optical emissions and striations induced by powerful HF radio waves at high latitudes: aspect angle dependence, J. Geophys. Res., 108, (A4), doi:10.1029/2002JA009543, 1141, 2003.

Robinson, T. R.: The heating of the high latitude ionosphere by high power radio waves, Phys. Rep., 179, 2/3, 79–209, 1989.

Stubbe, P.: Review of ionospheric modification experiments at Tromsø, J. Atmos. Terr. Phys., 58, 349–368, 1996.

Tereshchenko, E. D., Khudukon, B. Z., Rietveld, M. T., and Brekke, A.: Spatial structure of auroral day-time ionospheric electron density irregularities generated by a powerful HF-wave, Ann. Geophys., 16, 812–820, 1998, http://www.ann-geophys.net/16/812/1998/.

Tereshchenko, E. D., Khudukon, B. Z., Kozlova, M. O., and Nygrén, T.: Anisotropy of ionospheric irregularities determined from the amplitude of satellite signals at a single receiver, Ann. Geophys., 17, 508–518, 1999, http://www.ann-geophys.net/17/508/1999/.

Tereshchenko, E. D., Kozlova, M. O., Evstafjev, O. V., Khudukon, B. Z., Nygrén, T., Rietveld, M. T., and Brekke, A.: Irregular structures of the F layer at high latitudes during ionospheric heating, Ann. Geophys.,18, 1197–1209, 2000a.

Tereshchenko, E. D., Khudukon, B. Z., Kozlova, M. O., Evstafiev, O. V., Nygrén, T., Rietveld, M. T., and Brekke, A.: Comparison of the orientation of small-scale electron density irregularities and F region plasma flow direction, Ann. Geophys., 18, 8, 918–927, 2000b.

Tereshchenko, E. D., Khudukon, B. Z., Gurevich, A. V., Zybin, K. P., Frolov, V. L., Myasnikov, E. N., Muravieva, N. V., and Carlson, H. C.: Radio tomography and scintillation studies of ionospheric electron density modification caused by a powerful HF-wave and magnetic zenith effect at mid-latitudes, Physics Letters A, 325, 381–388, 2004b.

Tereshchenko, E. D., Yurik, R. Yu., Khudukon, B. Z., Rietveld, M. T., Isham, B., Belyey, V. Brekke, A., Hagfors, T., and Grill, M.: Directional features of the downshifted peak observed in HF-induced stimulated electromagnetic emission spectra obtained using an interferometer, Ann. Geophys., 24, 1819–1827, 2006, http://www.ann-geophys.net/24/1819/2006/.